Available online at www.sciencedirect.com
SCIENCE DIRECT®
Journal of Solid State Chemistry 179 (2006) 111–116
JOURNAL OF SOLID STATE CHEMISTRY
www.elsevier.com/locate/jssc

Electron-doping through La^{III}-for-Sr^{II} substitution in $(Sr_{1-x}La_x)_2FeTaO_6$: Effects on the valences and ordering of the *B*-site cations, Fe and Ta

E.-L. Rautama[a,b], T.S. Chan[c], R.S. Liu[c], J.M. Chen[d], H. Yamauchi[a], M. Karppinen[a,*]

[a]*Materials and Structures Laboratory, Tokyo Institute of Technology, 4259 Nagatsuta, Midori-ku, Yokohama 226-8503, Japan*
[b]*Laboratory of Inorganic and Analytical Chemistry, Helsinki University of Technology, FIN-02015 HUT, Finland*
[c]*Department of Chemistry and Center for Nano Storage Research, National Taiwan University, Taipei, Taiwan, Republic of China*
[d]*National Synchrotron Radiation Research Center, Hsinchu, Taiwan, Republic of China*

Received 18 August 2005; received in revised form 4 October 2005; accepted 5 October 2005
Available online 11 November 2005

Abstract

We have employed aliovalent *A*-site cation substitution, La^{III}-for-Sr^{II}, to dope the $Sr(Fe_{0.5}Ta_{0.5})O_3$ perovskite oxide with electrons. Essentially single-phase samples of $(Sr_{1-x}La_x)(Fe_{0.5}Ta_{0.5})O_3$ were successfully synthesized up to $x \approx 0.3$ in a vacuum furnace at 1400 °C. The samples were found to crystallize (rather than with orthorhombic symmetry) in monoclinic space group $P2_1/n$ that accounts for the partial ordering of the *B*-site cations, Fe and Ta. With increasing La-substitution level, *x*, the degree of Fe/Ta order was found to increase such that the La-richest compositions are best described by the *B*-site ordered double-perovskite formula, $(Sr,La)_2FeTaO_6$. From Fe L_3 and Ta L_3 XANES spectra it was revealed that upon electron doping the two *B*-site cations, Fe^{III} and Ta^{V}, are both prone to reduction. Magnetic susceptibility measurements showed spin-glass type behaviour for all the samples with a transition temperature slightly increasing with increasing *x*.

Keywords: Double perovskite; Cation ordering; Valence states; XANES spectroscopy

1. Introduction

The *B*-site ordered double-perovskite (DP) structure of the compounds, $A_2B'B''O_6$, is derived from that of the single-perovskite (SP) compounds, ABO_3, upon co-occupation of the octahedral cation site with two different metal species, B' and B'', in an ordered manner, such that each $B'O_6$ octahedron is surrounded by six corner-sharing $B''O_6$ octahedra, and vice versa. The ideal face-centred cubic unit cell of a *B*-site ordered DP is $2 \times 2 \times 2 = 8$ times larger than the primitive cubic cell of the SP that corresponds to the disordered case. The DP compound family has been intensively revisited since the discovery of room-temperature half-metallicity and tunnelling-type magnetoresistance effect in Sr_2FeMoO_6 [1], Sr_2FeReO_6 [2] and many other ferri/ferromagnetic $A_2Fe(Mo,Re)O_6$ (A = Ca, Sr, Ba) compounds. As a common crystal-chemical feature, these compounds have been found to possess not only (i) high degree of order, but also (ii) valence mixing between the *B*-site cations, Fe and Mo/Re [3–9].

The high degree of order in $A_2B'B''O_6$ is achieved only if the charge difference between the *B* cations is large enough [10]. Accordingly only the $A_2B'^{I}B''^{VII}O_6$ and $A_2B'^{II}B''^{VI}O_6$-type compounds are usually perfectly ordered, whereas among the $A_2B'^{III}B''^{V}O_6$ compounds various levels of ordering are observed. For the latter case, the degree of order is known to strongly depend on the synthesis conditions [10,11], but it also depends on the particular A, B' and B'' cations. Empirically for many of the known systems the degree of order of the *B* cations increases when the size of the *A* cation decreases [10].

The valence mixing between the B' and B'' cations depends also on multiple factors. In the prototype DP

*Corresponding author. Fax: +81 45 924 5365.
E-mail address: karppinen@msl.titech.ac.jp (M. Karppinen).

0022-4596/$ - see front matter © 2005 Elsevier Inc. All rights reserved.
doi:10.1016/j.jssc.2005.10.004

half-metal, Sr_2FeMoO_6, the itinerant d electron of formally pentavalent Mo ($4d^1$) transfers part of its charge and spin to formally trivalent Fe ($3d^5$), and as a consequence the mixed-valence states, $Fe^{II/III}$ and $Mo^{V/VI}$, are realized. The precise charge balance between Fe and Mo is then controlled by, e.g. the choice (= average size) of the A-site cation constituent [9,12–14]. In partially disordered samples the valence mixing is hindered: the misplaced Fe (and Mo) atoms with Fe (Mo) rather than Mo (Fe) atoms as nearest-neighbour B cations possess integer rather than mixed valence value, as probably most directly revealed from ^{57}Fe Mossbauer spectra for such samples [3,5,9,15]. Hence it seems that the degree of order and the valence mixing (and thereby even the metallicity/half-metallicity) are strongly linked characteristics for the $A_2Fe(Mo,Re)O_6$-type compounds.

The aim of the present work was to find new potential candidates for half-metallic DP oxides. The SP oxide, $Sr(Fe_{0.5}Ta_{0.5})O_3$ with trivalent Fe ($3d^5$) and pentavalent Ta ($5d^0$) [7,8], was selected for the target system. The strategy was set so as to dope the system through aliovalent La^{III}-for-Sr^{II} substitution with additional electrons, which then might be shared by the two B-site cations, Fe and Ta, to facilitate mixed-valence states for both of them. X-ray absorption near-edge structure (XANES) spectroscopy and X-ray diffraction (XRD) techniques were utilized for sample characterization in terms of the valence states and ordering of Fe and Ta, respectively. Magnetic properties were evaluated on the basis of SQUID (superconducting quantum interference device) measurements.

2. Experimental

A series of samples of the $(Sr_{1-x}La_x)_2FeTaO_6$ system was synthesized by means of solid-state reaction from stoichiometric mixtures of high-purity (99.9%) powders of $SrCO_3$, La_2O_3, Fe_2O_3 and Ta_2O_5. The La_2O_3 powder was fired in air at 1000 °C for 24 h and checked for phase purity before accurate weighing. The powder mixture was calcined in air at 1000 °C for 24 h. The calcined powder was pelletized and sintered in a high-temperature vacuum furnace in alumina crucibles at 1400 °C for 20–30 h. The time required for successful synthesis was found to increase with increasing La substitution level, x. The phase purity of the samples was confirmed by X-ray powder diffraction (Rigaku RINT-2500 V equipped with a rotating anode; Cu K_α radiation). The lattice parameters and the fractional occupancies of Fe and Ta at the two B-cation sites (of the DP structure) were determined from the XRD data by means of Rietveld refinement using the refinement software, RIETAN 2000 [16]. The data for the refinements were collected using a large-window sample holder (200 mm × 170 mm) in the range of $15° \leqslant 2\theta \leqslant 120°$ with a measurement step of 0.02° and counting for 1 s at each step.

Oxygen content was determined cerimetrically for two representative samples, $x = 0.0$ and 0.2. A precisely weighed specimen of 15–20 mg of sample powder was dissolved in 120 ml of 9 M HCl solution in a beaker under Ar flow aided by stirring and heating. After the sample was completely dissolved, the solution was rapidly cooled back to room temperature and the titration of the possibly existing reduced species of Fe^{2+} and/or Ta^{4+} was performed (after adding 15 ml of concentrated phosphoric acid to act as a complexant for Fe^{3+}) with 0.008 M $Ce(SO_4)_2$ solution (standardized against Mohr's salt) using ferroin as an indicator. Blank experiments were found essentially important to be able to take into account the unfavorable but unavoidable redox reaction between Cl^- and Fe^{3+} in concentrated HCl solutions; these experiments were carried out using Fe_2O_3 as a source of Fe^{3+} and following exactly the same sample solution and titration procedure as used in the actual titration experiments. Each titration experiment was repeated three times in minimum with a good reproducibility (better than ± 0.005 for the final oxygen content).

Changes in the valence states of the two B cations, Fe and Ta, upon electron doping were probed by Fe L_3- and Ta L_3-edge XANES spectroscopy experiments carried out at the National Synchrotron Radiation Research Center (NSRRC) in Hsinchu, Taiwan, with an electron beam energy of 1.5 GeV and a maximum stored current of 240 mA [8,13]. All the measurements were performed at room temperature. The Ta L_3-edge XANES spectra were recorded in transmission mode using gas-filled ionization chambers at the multipole Wiggler beamline BL17C. The ion chambers used for measuring the incident (I_0) and the transmitted beam intensities were filled with a mixture of N_2 and H_2 gases and a mixture of N_2 and Ar gases, respectively. The sample was ground to pass through a 400-mesh sieve to fulfill the requirement that the size of the particles is smaller than the absorption length in the material, i.e. $\mu d < 1$, where d is the particle size and μ is the total absorption coefficient. The resultant fine powder was rubbed homogeneously onto Scotch tape. Then the thickness of the sample was carefully adjusted by folding the Scotch tape several times to achieve $\Delta\mu x \approx 1$, where $\Delta\mu x$ is the edge step. The Fe L_3-edge spectra were recorded by measuring the sample drain current in an ultrahigh vacuum chamber (10^{-9} Torr) at the 6-m high-energy spherical grating monochromator (HSGM) beamline BL20A. The incident photon flux (I_0) was monitored simultaneously by using a Ni mesh located after the exit slit of the monochromatic beam. All the absorption measurements were normalized to I_0.

Magnetization measurements were performed both in zero-field-cooled (ZFC) and field-cooled (FC) modes (10 Oe; 5–400 K) using a SQUID magnetometer (Quantum Design MPMSR-5S).

3. Results and discussion

The $(Sr_{1-x}La_x)_2FeTaO_6$ samples were found to be of single phase up to the La-substitution level of $x = 0.3$. For

samples with the higher La contents traces of La_3TaO_7 were detected in the X-ray diffraction patterns. Oxygen-content analysis carried out for the two representative samples of $x = 0.0$ and 0.2 gave values of 5.995(5) and 5.997(5), respectively, for the oxygen content *per* formula unit. Hence, we conclude that our $(Sr_{1-x}La_x)_2FeTaO_6$ samples are essentially stoichiometric.

The parent Sr_2FeTaO_6 compound has previously been reported to crystallize with the orthorhombic *Pbnm* (No. 62) space group [17] that is compatible with random distribution of Fe and Ta at the *B*-cation site [7,8,17], i.e. the SP structure. X-ray diffraction patterns for the present samples revealed weak super-cell reflections due to partial *B* cation ordering even for the non-substituted Sr_2FeTaO_6 sample; then with increasing La-substitution level x, the Bragg peaks representing doubled unit-cell axis lengths gradually got strengthened. The reason for the first observation is probably the higher synthesis temperature employed here which enhances the speed of the otherwise sluggish cation ordering process at the perovskite *B* site [11,17]. Similar results were obtained by Tao et al. [18] in the case of Sr_2FeNbO_6.

A monoclinic space group $P2_1/n$ (No. 14), that is a subgroup of *Pbnm* allowing the (three-dimensional) doubling of the unit cell [19,20], was considered to be the best candidate for the structural model of the present samples. This is because there is no valid orthorhombic space group for a *B*-site ordered DP with $\sim\sqrt{2}a_p \times \sim\sqrt{2}a_p \times \sim 2a_p$ unit cell, but the resulting symmetry originating from the orthorhombic octahedral tilting is monoclinic [19,21]. Structures of the higher symmetries could be excluded on the basis of peak splitting occurring in the high-2θ region which would not appear in, e.g. a tetragonal structure. The starting point for the Rietveld refinement in terms of lattice parameters and atomic positions was constructed employing the software SPuDS [22]. In total 42 parameters were refined, and the quality of the fitting turned out to be good, with R_{wp} values clearly lower than 10% for all the single-phase samples investigated. The XRD patterns for the $x = 0.0$ and 0.2 samples together with corresponding Rietveld fitting profiles are presented in Figs. 1(a) and (b), respectively. The inset in Fig. 1(a) shows a magnification of the peak splitting at $2\theta \approx 100^\circ$. The resultant structural parameters for four samples with $x = 0.0$, 0.1, 0.2 and 0.3 are given in Table 1. Even though the structure is monoclinic, the distortion angle β was found to differ only slightly from 90°, such that the structure in practice is nearly orthorhombic. It should be mentioned that we also attempted to refine the $x = 0.0$ sample in the space group *Pbnm*. However, the result was not satisfactory as some of the peaks were slightly shifted from their calculated positions and the R_{wp} value remained as high as 28%. With increasing La-for-Sr substitution level, the cell volume was found to increase (see the inset of Fig. 1(b)), although the magnitude of the change is minimal. This is due to the fact that the substitution causes two phenomena simultaneously that work opposite to each other, i.e. the

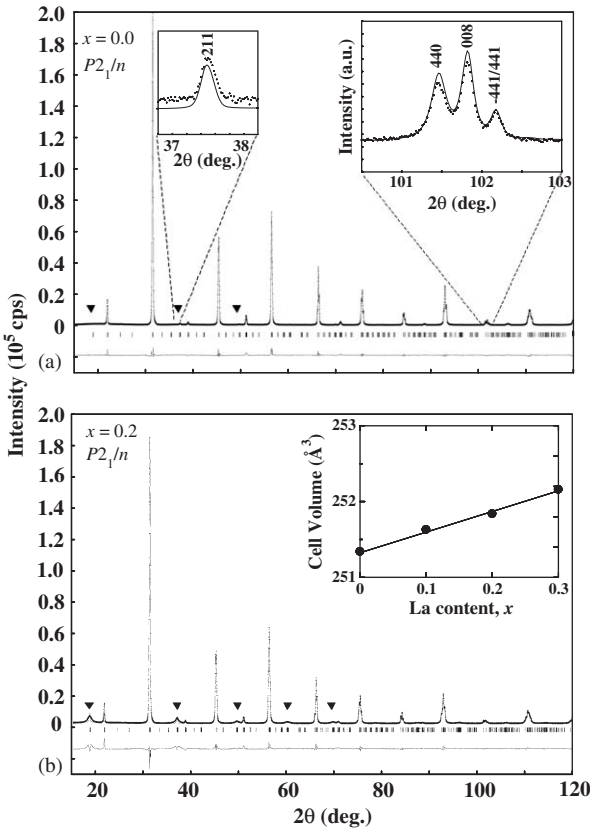

Fig. 1. Observed (dots) and calculated (solid) room-temperature X-ray powder diffraction profiles of $(Sr_{1-x}La_x)_2FeTaO_6$ with (a) $x = 0.0$, and (b) $x = 0.2$. The vertical lines indicate the positions of the allowed Bragg reflections. The difference curve, I_{obs}–I_{calc}, is shown at the bottom. The insets in (a) show magnifications of the 2θ areas of 37–38° and 101–103° to emphasize, respectively, the presence of supercell peaks and monoclinic distortion. The cell volume as a function of x is shown in the inset of (b). The supercell peaks are marked with arrows.

size of the La^{III} ion is smaller than that of Sr^{II} so that the substitution should decrease the cell volume, and at the same time La reduces the average valence of the *B* cations, thus increasing their ionic radii.

As an indication of the increasing degree of long-range ordering with increasing La-substitution level, the relative intensities of the super-cell reflections were found to increase, but at the same time these peaks became broader than the fundamental peaks, which somewhat lowered the quality of the fitting (see the trend in quality-of-fit parameters in Table 1). (This latter point is common to partially ordered DP samples in which the ordered domains are smaller than the crystallites [10].) The refined fractional occupancies (g) of Fe and Ta at the two *B* sites were used to calculate the long-range order parameter (S) as: $S = 2(g_{Fe}–0.5)$. Special attention was paid to refine these occupancies as reliably as possible. The strategy was as follows: in the beginning the fractional occupancies of the two *B* cations, Fe and Ta, were set to 0.5 each, i.e. assuming no ordering between them. The isotropic thermal parameters (B) were initially fixed to appropriate values, i.e. 0.3–0.5 for the cations and 0.8 for the lighter oxygen

Table 1
Lattice parameters and atomic positions for the $(Sr_{1-x}La_x)_2FeTaO_6$ samples obtained from X-ray diffraction profiles through Rietveld refinement in space group $P2_1/n$ (No. 14)

La content, x	0.0	0.1	0.2	0.3
a (Å)	5.6201(7)	5.6199(2)	5.6206(2)	5.6235(1)
b (Å)	5.6343(7)	5.6416(2)	5.6445(2)	5.6448(2)
c (Å)	7.9375(7)	7.9365(2)	7.9381(2)	7.9436(2)
β (deg)	89.99(1)	89.98(3)	89.97(2)	89.97(6)
Sr/La (4*e*)				
x	0.5076(8)	0.4888(6)	0.5174(6)	0.5143(7)
y	0.5078(4)	0.4931(7)	0.4908(7)	0.508(1)
z	0.2532(8)	0.251(1)	0.2571(7)	0.251(2)
B (in Å^2)	0.48	0.42	0.44	0.44
Fe(1)(2*c*)				
g	0.53	0.60	0.72	0.80
B (in Å^2)	0.51	0.55	0.50	0.58
Ta(1) (2*d*)				
g	0.53	0.60	0.72	0.80
B (in Å^2)	0.55	0.48	0.36	0.46
O(1) (4*e*)				
x	0.24(1)	0.266(6)	0.235(7)	0.25(1)
y	0.244(8)	0.29(1)	0.247(9)	0.26(1)
z	−0.01(1)	−0.016(9)	0.011(9)	−0.002(9)
O(2) (4*e*)				
x	0.268(5)	0.283(7)	0.283(7)	0.25(1)
y	0.721(5)	0.750(9)	0.750(9)	0.73(1)
z	−0.005(8)	0.01(1)	0.016(9)	−0.024(6)
O(3) (4*e*)				
x	0.470(5)	0.490(4)	0.505(4)	0.428(6)
y	0.002(2)	0.001(3)	0.004(4)	0.035(6)
z	0.250(7)	0.241(3)	0.243(4)	0.252(4)
R_{wp} (%)	7.66	8.52	9.89	9.87
R_p (%)	5.82	6.22	6.69	7.40
χ^2	3.98	4.56	5.32	4.98

Sr/La at (x, y, z), Fe(1)/Ta(2) at (0, 0.5, 0), Ta(1)/Fe(2) at (0.5, 0, 0) and O(1)–O(3) at (x, y, z).

atoms. For the very poorly ordered samples ($x = 0.0$ and 0.1) the fractional occupancies were released just before starting the refinement of the atomic positions, whereas for $x = 0.2$ and 0.3 they were refined earlier, after the cell parameters and before the peak-shape parameters (although it seemed that the order did not have any significant effect). Thermal parameters were released at the final stage of each refinement. However, it turned out that it is necessary to fix the thermal parameters of oxygen atoms, since releasing them resulted in unacceptable values. From Table 1, the refined occupancy of Fe at its proper site is: $g_{Fe} = 0.53$, 0.60, 0.72 and 0.80 for $x = 0.0$, 0.1, 0.2 and 0.3, respectively. In Fig. 2, the corresponding values of the long-range order parameter S are plotted against the La content, x.

Fig. 3(a) shows the L_3 portion of the Fe L-edge XANES spectra for a series of $(Sr_{1-x}La_x)_2FeTaO_6$ samples with $x = 0.0-0.3$, together with spectra for the reference

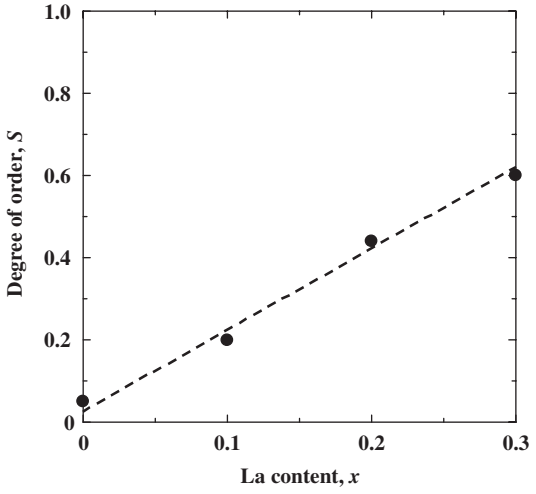

Fig. 2. Degree of B-site cation order (S) plotted against the La-substitution level (x) for the $(Sr_{1-x}La_x)_2FeTaO_6$ samples.

materials Fe_2O_3 (six-coordinated trivalent Fe) and $Sr_2Fe(W_{0.9}Mo_{0.1})O_6$ (six-coordinated divalent Fe) [8]. The main spectral features of the L edge of Fe originate from dipole transitions from the core Fe $2p$ level to the empty Fe $3d$ states, and are separated into two regions due to the core–hole spin–orbit interaction: Fe $2p_{3/2}$ (L_3 edge; 705–715 eV) and Fe $2p_{1/2}$ (L_2 edge; 715–730 eV) [8,12,13,23]. (The weaker $2p \rightarrow 4s$ transitions contribute only to the smooth background at high energies.) Due to the weakness of the L_2 area, only the Fe L_3 edge was used in the analysis. The L_3 edge is further divided into two peaks. The splitting and the intensity ratio between them are determined by the interplay of crystal-field effects and electronic interactions. The L_3 absorption edge of Fe^{III} species in an octahedral crystal field typically exhibits a main peak at the higher-energy side (~709 eV), with a weaker peak or a shoulder at the lower energy (~707 eV) [8,12,13,23], see for example the spectrum of Fe_2O_3 in Fig. 3(a). The order of the peaks is reverse for Fe^{II} species, e.g. in $Sr_2Fe(W_{0.9}Mo_{0.1})O_6$ (Fig. 3(a)). For the non-substituted Sr_2FeTaO_6 sample the intensity of the higher-energy peak (I_{709}) is clearly higher than that of the lower-energy peak (I_{707}) as a manifestation of the trivalent state of Fe in this sample. With increasing La^{III}-for-Sr^{II} substitution level, i.e. electron doping, the intensity ratio, I_{709}/I_{707}, decreases indicating that the valence state of Fe decreases; in Fig. 3(b) the intensity ratio is plotted against x. From Fig. 3(a) it also seems that with decreasing Fe valence the energy separation of the two L_3 peaks slightly increases.

As for the Ta L_3 edge, the XANES spectra in Fig. 4(a) show that the absorption edge is gradually shifting to the lower-energy side as the level of La substitution increases. Since the absorption energy corresponds to the valence state such that the higher the absorption energy, the higher the valence value, the result proves that the valence of Ta is also slightly decreasing (from pentavalency somewhat

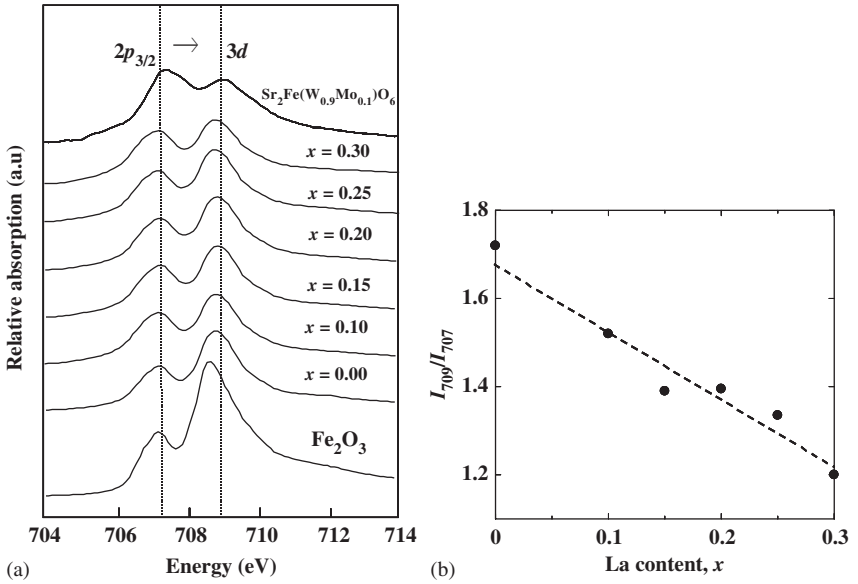

Fig. 3. (a) Fe L_3 XANES spectra for $(Sr_{1-x}La_x)_2FeTaO_6$ ($0.0 \leqslant x \leqslant 0.3$) samples in the energy range of 704–714 eV, and (b) the intensity ratio, I_{709}/I_{707}, of the two peaks at ~707 and ~709 eV plotted against the La substitution level, x. Also shown in (a) are spectra for Fe_2O_3 (Fe^{III}) and $Sr_2Fe(W_{0.9}Mo_{0.1})O_6$ (Fe^{II}) [8] for reference.

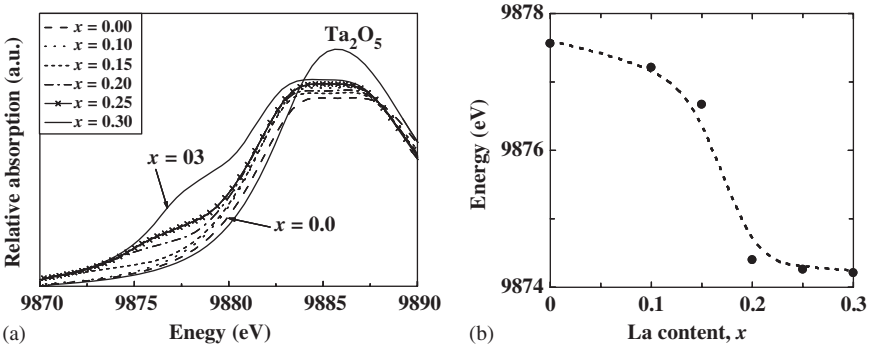

Fig. 4. (a) Ta L_3 XANES spectra for $(Sr_{1-x}La_x)_2FeTaO_6$ ($0.0 \leqslant x \leqslant 0.3$) samples in the energy range of 9870–9890 eV, and (b) energy of the absorption edge plotted against the La substitution level, x. Also shown is a spectrum for Ta_2O_5 (Ta^V) for reference.

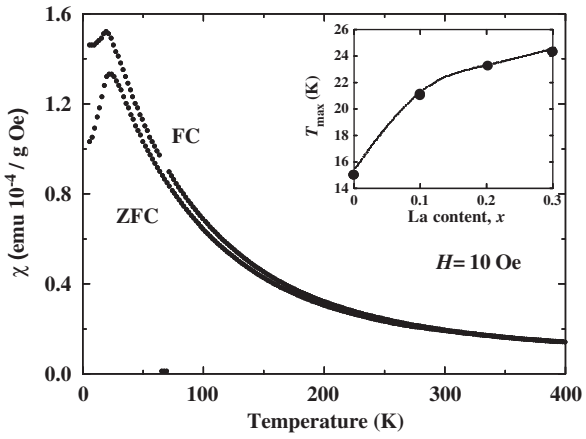

Fig. 5. Typical magnetic susceptibility (χ) versus temperature behaviour observed for the $(Sr_{1-x}La_x)_2FeTaO_6$ system, here shown for the $x = 0.2$ sample. The inset shows the dependence of the susceptibility maxima (T_{max}) on the La substitution level, x.

towards tetravalency) upon increasing the electron-doping level in $(Sr_{1-x}La_x)_2FeTaO_6$ through La substitution. The decrease in absorption energy is illustrated in Fig. 4(b).

The parent Sr_2FeTaO_6 phase has been reported to be a spin glass in an earlier study [17]. From the present magnetic susceptibility measurements a similar spin-glass-type behaviour was seen for La-substituted $(Sr_{1-x}La_x)_2FeTaO_6$ samples too, with a slightly increasing susceptibility-maximum temperature (T_{max}) with increasing La-substitution level. Fig. 5 depicts the ZFC and FC magnetic susceptibility curves for the $x = 0.2$ sample, and the inset shows the dependence of the value of T_{max} on the substitution level, x.

4. Conclusions

A series of single-phase $(Sr_{1-x}La_x)_2FeTaO_6$ samples up to $x = 0.3$ was prepared here for the first time. The thus

achieved (at least nominally) electron-doped compounds were found to possess a double perovskite structure with monoclinic $P2_1/n$ symmetry and partial ordering between the *B*-site cations, Fe and Ta. With increasing x, the long-range ordering got markedly enhanced, whereas the magnetic properties remained essentially the same, i.e. the spin-glass behaviour previously reported for the pristine Sr_2FeTaO_6 phase was found to be preserved up to the highest La-substitution level achieved. From XANES spectroscopy experiments involving the L_3 edges of Fe and Ta, revealed was valence-state reduction for both Fe and Ta as the electron-doping level increased in overall, thereby providing us with promising evidence towards successful creation of mixed valence states for the two *B*-site cations in $(Sr,La)_2FeTaO_6$.

Acknowledgments

Prof. Pavel Karen of University of Oslo is thanked for his guidance in crystal structure analyses. This work was supported by Grants-in-aid for Scientific Research (Nos. 15206002 and 15206071) from the Japan Society for the Promotion of Science. E.-L.R. acknowledges the support from the Scandinavia–Japan Sasakawa Foundation and T.S.C. and R.S.L. from the Ministry Economic Affairs of Taiwan (under the grant number 94-EC-17-A-08-S1-0006).

References

[1] K.-I. Kobayashi, T. Kimura, H. Sawada, K. Terakura, Y. Tokura, Nature 395 (1998) 677.
[2] K.-I. Kobayashi, T. Kimura, Y. Tomioka, H. Sawada, K. Terakura, Y. Tokura, Phys. Rev. B 59 (1999) 11159.
[3] J. Lindén, T. Yamamoto, M. Karppinen, H. Yamauchi, T. Pietari, Appl. Phys. Lett. 76 (2000) 2925.
[4] O. Chmaissem, R. Kruk, B. Dabrowski, D.E. Brown, X. Xiong, S. Kolesnik, J.D. Jorgensen, C.W. Kimball, Phys. Rev. B 62 (2000) 14197.
[5] J.M. Grenèche, M. Venkatesan, R. Suryanarayanan, J.M.D. Coey, Phys. Rev. B 63 (2001) 174403.
[6] J. Gopalakrishnan, A. Chattopadhyay, S.B. Ogale, T. Venkatesan, R.L. Greene, A.J. Millis, K. Ramesha, B. Hannoyer, G. Marest, Phys. Rev. B 62 (2000) 9538.
[7] J. Lindén, T. Yamamoto, J. Nakamura, H. Yamauchi, M. Karppinen, Phys. Rev. B 66 (2002) 184408.
[8] M. Karppinen, H. Yamauchi, Y. Yasukawa, J. Lindén, T.S. Chan, R.S. Liu, J.M. Chen, Chem. Mater. 15 (2003) 4118.
[9] Y. Yasukawa, J. Lindén, T.S. Chan, R.S. Liu, H. Yamauchi, M. Karppinen, J. Solid State Chem. 177 (2004) 2655.
[10] P. Woodward, R.-D. Hoffmann, A.W. Sleight, J. Mater. Res. 9 (1994) 2118.
[11] T. Shimada, J. Nakamura, T. Motohashi, H. Yamauchi, M. Karppinen, Chem. Mater. 15 (2003) 4494;
Y.H. Huang, J. Lindén, H. Yamauchi, M. Karppinen, Chem. Mater. 16 (2004) 4337.
[12] J.-S. Kang, J.H. Kim, A. Sekiyama, S. Kasai, S. Suga, S.W. Han, K.H. Kim, T. Muro, Y. Saitoh, C. Hwang, C.G. Olson, B.J. Park, B.W. Lee, J.H. Shim, J.H. Park, B.I. Min, Phys. Rev. B 66 (2002) 113105.
[13] T.S. Chan, R.S. Liu, G.Y. Guo, S.F. Hu, J.G. Lin, J.M. Chen, J.P. Attfield, Chem. Mater. 15 (2003) 425.
[14] J. Herrero-Martin, J. Garcia, G. Subias, J. Blasco, M.C. Sanchez, J. Phys. Cond. Mater. 16 (2004) 6877.
[15] J. Lindén, T. Shimada, T. Motohashi, H. Yamauchi, M. Karppinen, Solid State Commun. 129 (2003) 129.
[16] F. Izumi, T. Ikeda, Mater. Sci. Forum 321–324 (2000) 198.
[17] P.D. Battle, T.C. Gibb, A.J. Herod, S.-H. Kim, P.H. Munns, J. Mater. Chem. 5 (1995) 865;
E.J. Cussen, J.F. Vente, P.D. Battle, T.C. Gibb, J. Mater. Chem. 7 (1997) 459.
[18] S. Tao, J. Canales-Vázquez, J.T.S. Irvine, Chem. Mater. 16 (2004) 2306.
[19] C.J. Howard, B.J. Kennedy, P.M. Woodward, Acta Crystallogr. B 59 (2003) 463.
[20] J.A. Alonso, M.T. Casais, M.J. Martínez-Lope, J.L. Martínez, P. Velasco, A. Muñoz, M.T. Fernández-Díaz, Chem. Mater. 12 (2000) 161.
[21] P.M. Woodward, Acta Crystallogr. B 53 (1997) 32.
[22] M.W. Lufaso, P.M. Woodward, Acta Crystallogr. B 57 (2001) 725.
[23] J.P. Crocombette, M. Pollak, F. Jollet, N. Thromat, M. Gautier-Soyer, Phys. Rev. B 52 (1995) 3143.